

## COMMUNICATION



# What is the thermal conductivity limit of silicon germanium alloys?<sup>†</sup>

 Yongjin Lee,<sup>‡</sup> Alexander J. Pak<sup>‡</sup> and Gyeong S. Hwang\*

 Cite this: *Phys. Chem. Chem. Phys.*, 2016, 18, 19544

 Received 23rd June 2016,  
Accepted 5th July 2016

DOI: 10.1039/c6cp04388g

[www.rsc.org/pccp](http://www.rsc.org/pccp)

The lowest possible thermal conductivity of silicon–germanium (SiGe) bulk alloys achievable through alloy scattering, or the so-called alloy limit, is important to identify for thermoelectric applications. However, this limit remains a subject of contention as both experimentally-reported and theoretically-predicted values tend to be widely scattered and inconclusive. In this work, we present a possible explanation for these discrepancies by demonstrating that the thermal conductivity can vary significantly depending on the degree of randomness in the spatial arrangement of the constituent atoms. Our study suggests that the available experimental data, obtained from alloy samples synthesized using ball-milling techniques, and previous first-principles calculations, restricted by small supercell sizes, may not have accessed the alloy limit. We find that low-frequency anharmonic phonon modes can persist unless the spatial distribution of Si and Ge atoms is completely random at the atomic scale, in which case the lowest possible thermal conductivity may be achieved. Our theoretical analysis predicts that the alloy limit of SiGe could be around  $1\text{--}2\text{ W m}^{-1}\text{ K}^{-1}$  with an optimal composition around 25 at% Ge, which is substantially lower than previously reported values from experiments and first-principles calculations.

## 1. Introduction

Silicon–germanium (SiGe) alloys are promising candidate materials for thermoelectric (TE) energy conversion. The main reason is their low thermal conductivity ( $\kappa$ ), due to significant phonon scattering by alloying (or so-called alloy scattering), as the TE efficiency is inversely proportional to  $\kappa$ . Good TE materials must have a low  $\kappa$  and excellent electronic transport properties, as characterized by the dimensionless figure of merit  $ZT (=S^2\sigma T/\kappa)$ , where  $S$  is the

Seebeck coefficient,  $\sigma$  is the electrical conductivity, and  $T$  is the absolute temperature). Theoretical studies have identified that alloy scattering in SiGe is mainly induced by mass disorder among constituent atoms,<sup>1,2</sup> a type of intrinsic scattering. As a result, experimental efforts have attempted to facilitate further reduction of  $\kappa$  by incorporating extrinsic scattering through nanostructuring.<sup>3–7</sup> However, an understanding of the conditions that maximize the mass disorder effect should be undertaken to find the corresponding lowest  $\kappa$  of SiGe, or the so-called alloy limit.

Previous experimentally reported values for the alloy limit of SiGe have been inconclusive. For instance, the  $\kappa$  of  $\text{Si}_{0.8}\text{Ge}_{0.2}$  has been reported to range from 5 to  $15\text{ W m}^{-1}\text{ K}^{-1}$ .<sup>8–13</sup> Also, while various theoretical methods have been successfully employed to understand the underlying mechanisms of heat transport in SiGe alloys,<sup>1,14–19</sup> the large variation of predicted thermal conductivities among different methods underscores the necessity to assess the reliability of these various computational conditions. For instance, solutions to the Boltzmann transport equation using the single-mode relaxation time approximation (BTE-RTA)<sup>1,14</sup> and virtual crystal approximation<sup>15</sup> based off of density functional theory (DFT) calculations and molecular dynamics (MD) calculations<sup>16–19</sup> give significantly different values for  $\kappa$  of SiGe even at the same alloy composition (e.g., the  $\kappa$  of  $\text{Si}_{0.8}\text{Ge}_{0.2}$  can range between 2 and  $10\text{ W m}^{-1}\text{ K}^{-1}$ ).

Meanwhile in our recent study,<sup>17</sup> it was shown that the strength of alloy scattering is significantly affected by atomic arrangement even at the same alloy composition. Noting that experimentally measured samples were mostly obtained *via* mechanical alloying (ball milling) of Si and Ge chunks, the prepared alloys may not be completely disordered and can contain a certain degree of ordering. Hence, the possible differences in atomic arrangements due to preparation conditions may explain the significant variation in  $\kappa$  from sample to sample. In a similar fashion, the discrepancies in  $\kappa$  for different theoretical methods might originate from the atomic arrangements considered within MD and DFT simulations. It would therefore be instructive to explore the sensitivity of predicted  $\kappa$  values to differences in the atomic arrangement of a given alloy

McKetta Department of Chemical Engineering, University of Texas, Austin, Texas 78712, USA. E-mail: gshwang@che.utexas.edu

<sup>†</sup> Electronic supplementary information (ESI) available: Full details on the computational methods and figures depicting mode-specific phonon group velocities and lifetimes. See DOI: 10.1039/c6cp04388g

<sup>‡</sup> The authors equally contributed to this work.

composition within similar supercell sizes. Here, the chosen supercell size should be large enough to fully capture long-range phonon modes in order to correctly predict the  $\kappa$  of SiGe alloys.

One way to characterize the differences in the atomic arrangement of a nearly random alloy is by the length-scale of possible periodicity, or so-called quasi-periodicity. In extreme cases, the alloy could be described by the perpetual repetition of a smaller and truly random alloy (*i.e.*, a super-lattice), which may be considered the “unit cell” and is defined by its size.

In this work, we investigate the limits of  $\kappa$  suppression within SiGe alloys through analysis of the sensitivity between  $\kappa$  and the extent of quasi-periodicity. First, the variations of  $\kappa$  according to the size of the random alloy unit cell are investigated using classical molecular dynamics for a wide range of alloy compositions;  $\kappa$  can be separated into lattice and electronic contributions in semiconductors, but the latter is insignificant in (undoped or lightly doped) SiGe alloys<sup>12</sup> and thus ignored in this study. Then, mode-specific phonon contributions to  $\kappa$  are computed and analyzed using time-domain normal mode analysis. Our analysis reveals that  $\kappa$  is strongly affected by atomic-scale randomness and only converges to a minimum value in the absence of quasi-periodicity throughout the lattice, thereby allowing anharmonic scattering of low-frequency (*i.e.*, long-range) phonon modes.

## II. Results and discussion

To tune the quasi-periodicity of the SiGe alloys (with  $\langle 100 \rangle$  orientation in  $x$ ,  $y$ , and  $z$ ), the size of the random alloy unit cell ( $N$ , corresponding to  $2^{3N}$  atoms) was varied as  $N = 1$  (8 atoms), 2 (64 atoms), 3 (512 atoms), 4 (4096 atoms), and 5 (32 768 atoms). Within each unit cell, Si and Ge atoms were randomly distributed using 12.5, 25, 50, and 87.5 at% Ge content. As depicted in Fig. 1, supercells were then constructed from the repetition of the unit cell (when  $N < 5$ ) such that all samples contained 32 768 atoms in a super-lattice configuration. The interatomic interactions were described using the Stillinger–Weber (SW) potential function with parameters that were re-optimized using a force-matching method<sup>20</sup> based on DFT calculations. All other computational details are provided in the ESI.†

Fig. 2 summarizes the computed variation of  $\kappa$  with  $N$  ( $=2^{3N}$  atoms) for  $\text{Si}_{1-x}\text{Ge}_x$  ( $x = 0.125, 0.25, 0.5, \text{ and } 0.875$ ) obtained from our EMD simulations using LAMMPS.<sup>21</sup> Our results confirm the following experimentally observed trends<sup>8–11</sup> (refer to open star symbols in Fig. 2):

- When  $x < 0.2$  (or  $x > 0.8$ ),  $\kappa$  rapidly drops as the Ge content increases (decreases)
- For  $0.2 < x < 0.8$ ,  $\kappa$  shows insignificant variation with  $x$
- The minimum value of  $\kappa$  occurs around  $x = 0.2$

Interestingly, the sensitivity of  $\kappa$  to  $N$  is clearly exhibited in Fig. 2. Specifically,  $\kappa$  monotonically decreases as  $N$  increases and converges beyond  $N = 4$  (inset of Fig. 2). When  $x = 0.25$ , for instance, the  $\kappa$  at  $N = 1$  ( $23.26 \text{ W m}^{-1} \text{ K}^{-1}$ ) is predicted to be about 15 times greater than the converged value of  $1.53 \text{ W m}^{-1} \text{ K}^{-1}$  at  $N = 4$ . In fact, this computed  $\kappa$  is found to be significantly lower

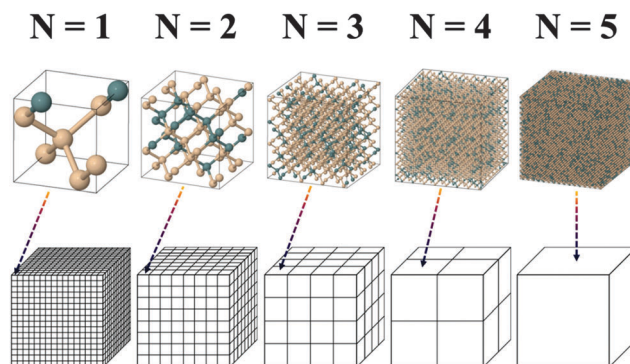


Fig. 1 Representative supercell structures of SiGe alloys with three dimensional periodic boundary conditions and 25 at% Ge content. The size of the repeating unit cell  $N$  (with  $2^{3N}$  atoms) varies from 1 to 5. When  $N < 5$ , the unit cell is repeated such that all structures contain 32 768 atoms. For different alloy compositions, lattice constants were adjusted according to Vegard's law.

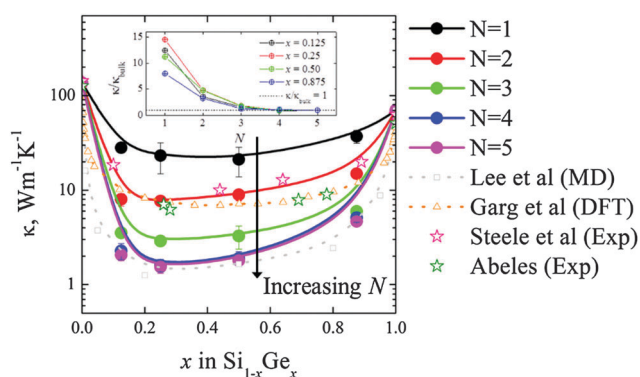


Fig. 2 Calculated thermal conductivities ( $\kappa$ ) of  $\text{Si}_{1-x}\text{Ge}_x$  ( $x = 0.125, 0.25, 0.5, \text{ and } 0.875$ ) for supercell size  $N = 1, 2, 3, 4, \text{ and } 5$  ( $N$  in  $2^{3N}$  atoms). Open gray squares<sup>17</sup> and orange triangles<sup>1</sup> represent previous NEMD and DFT results, respectively. Open star symbols represent experimental results.<sup>9,11</sup> The inset shows the normalized thermal conductivities ( $\kappa/\kappa_{\text{bulk}}$ ) of  $\text{Si}_{1-x}\text{Ge}_x$  as a function of  $N$ ; the black dashed line indicates  $\kappa = \kappa_{\text{bulk}}$ .

than previous experimentally reported values.<sup>8–11</sup> However, we do find that this converged value of  $\kappa$  is nearly identical to that predicted from our recent NEMD simulations which contained up to 64 000 randomly distributed Si/Ge atoms.<sup>17</sup> This suggests that the prediction of  $\kappa$  can be insensitive to the choice of MD technique as long as the system size is sufficiently large.

In Fig. 2, we also compare the predicted  $\kappa$  from *ab initio* BTE-RTA<sup>1</sup> to our EMD simulations and demonstrate a remarkably close agreement when  $N = 2$ ; for example at  $x = 0.5$ ,  $\kappa$  computed by Garg *et al.* from BTE-RTA is about  $7 \text{ W m}^{-1} \text{ K}^{-1}$  (using an explicit random lattice) which is similar to our calculated  $\kappa = 8.93 \text{ W m}^{-1} \text{ K}^{-1}$ . In their work, interatomic force constants up to third-order were extracted from DFPT calculations using 64-512 atom supercells, which were then used to estimate the anharmonic scattering rates. While Garg *et al.* demonstrated that the scattering rates of the phonon modes below 2 THz required explicitly random atomic arrangements (*i.e.*, the so-called virtual crystal approximation was insufficient to emulate these scattering events), they found that this system size achieved convergence.<sup>1</sup> In this work, we instead observe continuous

suppression of  $\kappa$  beyond  $N = 2$ . To investigate the influence of  $N$  further, we estimate the individual phonon mode contributions to thermal transport as discussed next.

We solve for the individual mode contributions to  $\kappa$  using the BTE-RTA method based on time-domain normal mode analysis (TDNMA) extracted from a combination of MD trajectories and anharmonic lattice dynamics, which can account for full anharmonicity (see the ESI†). Here, we consider the  $\text{Si}_{0.5}\text{Ge}_{0.5}$  alloy with  $N$  up to 4; as  $\kappa$  essentially converges beyond  $N = 4$ , the computationally expensive  $N = 5$  case is not considered such that all systems are limited to 4096 atoms. For comparison, we also include the zinc-blende alloy as this structure can be considered as an extreme case of a completely ordered alloy, which we find to have  $\kappa = 58.16 \pm 6.41 \text{ W m}^{-1} \text{ K}^{-1}$ ; the importance of the atomic arrangement can be noted by comparison to zinc-blende GaN which has a large  $\kappa \approx 100\text{--}250 \text{ W m}^{-1} \text{ K}^{-1}$  despite the mass difference between the two constituent atoms.<sup>22</sup> Fig. 3 depicts the estimated accumulation of  $\kappa$  as contributed by phonon modes of different frequencies  $\omega$ . First, it is clear that the  $\omega$  beyond which the accumulated  $\kappa$  saturates tends to decrease with increasingly disordered alloys (*i.e.*, from the ZB to  $N = 4$  cases). This demonstrates that the range of high-frequency phonon modes that are completed scattered tends to broaden as the atomic arrangement disorder increases, *i.e.*, as the regularity of the Si–Ge sub-lattice ordering is disrupted.

To account for the initial suppression of  $\kappa$  from the ZB to  $N = 1$  case, we refer to the computed phonon group velocities ( $v_g$ ) and mean free paths ( $L_{\text{MFP}}$ ) as shown in Fig. 4. A frequency gap is observed between 6.5 and 9.5 THz in the ZB case. The presence of the frequency gap restricts possible phonon scattering due to the necessity for energy and momentum conservation,<sup>23,24</sup> which has been similarly observed in other zinc-blende alloys including GaN and AlSb.<sup>25,26</sup> The existence of the frequency gap can be explained by a simple linear chain model.<sup>27</sup> For example, the diamond lattice can be described as a combination of

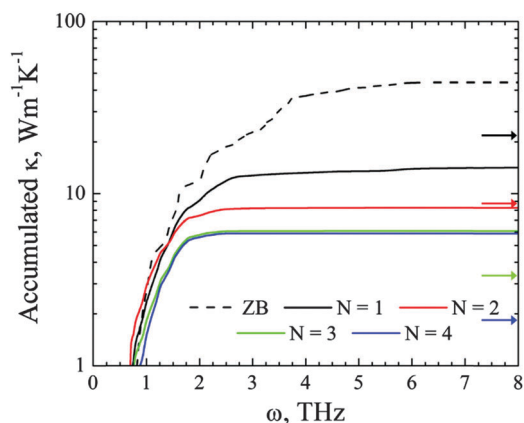


Fig. 3 Comparison of the accumulated thermal conductivity ( $\kappa$ ) with respect to phonon frequency ( $\omega$ ) for  $\text{Si}_{0.5}\text{Ge}_{0.5}$  with the listed atomic configurations using the BTE-RTA method based on time-domain normal mode analysis from MD trajectories. The predicted  $\kappa$  values from EMD calculations for each configuration are depicted by their respective colored arrows.

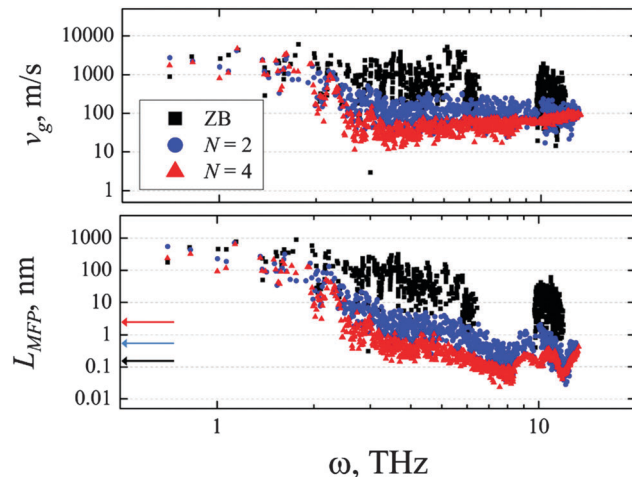


Fig. 4 Comparison of the phonon group velocity ( $v_g$ ) and mean free path ( $L_{\text{MFP}}$ ) for  $\text{Si}_{0.5}\text{Ge}_{0.5}$  in zinc-blende (ZB),  $N = 2$ , and  $N = 4$  configurations as a function of frequency ( $\omega$ ). The black, blue and red arrows indicate half the length of the simulation domain in the ZB,  $N = 2$ , and  $N = 4$  cases, respectively.

diatomic linear chains having two inequivalent lattice sites, such as Si and Ge, and two phonon branches (lower and upper). The highest frequency mode ( $\nu_{\text{H}}$ ) of the lower branches, associated with Si, and lowest frequency mode ( $\nu_{\text{L}}$ ) of the upper branches, associated with Ge, occur at the Brillouin zone boundaries. Due to the mass difference between Si and Ge,  $\nu_{\text{H}}$  and  $\nu_{\text{L}}$  have different frequencies and thereby results in a frequency gap. On the other hand, in the  $N = 1$  case, the two lattice sites are randomly occupied by either Si or Ge atoms. This therefore allows various eigenmodes to exist within the frequency gap, ultimately leading to  $\kappa$  suppression as a result of additional phonon scattering.

In Fig. 3, when  $N > 1$  our calculations find that the phonon modes below 2 THz are the dominant heat carriers. Therefore, as  $N$  increases, the reduction in  $\kappa$  can be attributed to the scattering of these low-frequency modes. Interestingly, the fact that our results predict further scattering of low-frequency phonons compared to that of ref. 1 seem to suggest that higher order anharmonics may be necessary to describe the low-frequency phonon behavior. However, we also find that our BTE-RTA results tend to overestimate (underestimate)  $\kappa$  when  $N > 2$  ( $N < 2$ ) compared to our EMD predictions. Given that the thermal conductivity of each mode is proportional to the mode-specific heat capacities,  $v_g$ , and  $L_{\text{MFP}}$ , we can qualitatively assess the accuracy of each. In general, we can assume that the least likely source of error is  $v_g$  (Fig. S1 and S2 in the ESI†) as this depends upon the stiffness of the Si–Si/Ge–Ge/Si–Ge bonds, which can be well-described by our parameterization of the SW force-field using the force-matching method. One possible source of error is our use of the quantum-harmonic heat capacity; previous studies have noted that the deviation in heat capacity between quantum-harmonic and classical-harmonic formalisms diminishes close to the Debye temperature while a significant deviation is seen with respect to the classical-anharmonic heat capacity.<sup>28</sup> However, we believe that the largest source of error is likely in the estimation of  $L_{\text{MFP}}$

(Fig. S1 and S2, ESI<sup>†</sup>) under the single-mode relaxation time approximation. The biggest drawback of this approximation is that collective or many-body scattering interactions between phonons are not explicitly accounted for, which may be increasingly important for long-range (*i.e.*, low-frequency) coupled modes. Furthermore, our TDNMA calculations may exacerbate this problem due to limitations in both our simulated system size and the description of many-body interactions in the force-field; both of these factors can allow long-range coupling of atomic vibrations to persist. Nonetheless, the TDNMA analysis demonstrates qualitatively that the anharmonic contribution to heat transport by the low-frequency phonon modes can be overestimated if quasi-periodicity exists (*i.e.*,  $N$  is too small). These findings highlight that the presence of microsegregation and/or quasi-periodicity (*i.e.*, super-lattice) in SiGe alloys can prevent the observation of the alloy-limit of  $\kappa$ .

### III. Conclusions

In summary, we investigated the lowest possible thermal conductivity ( $\kappa$ ) of SiGe alloys, or the so-called alloy limit, by assessing the sensitivity of  $\kappa$  to the randomness of the constituent atom arrangement throughout the alloy; this direction was motivated by our previous study<sup>17</sup> that demonstrated the sensitivity of  $\kappa$  at a given SiGe composition to the presence of locally segregated Si or Ge domains (or so-called microsegregation). In this work, we tuned the randomness by introducing quasi-periodicity through the construction of random-alloy superlattices with periodicity governed by the size of the unit cell used to describe the random atomic arrangement. Our molecular dynamics simulations showed that the predicted  $\kappa$  is inversely related to this unit cell size and converges to a minimum around  $1\text{--}2\text{ W m}^{-1}\text{ K}^{-1}$  in the  $\text{Si}_{0.75}\text{Ge}_{0.25}$  alloy. Detailed phonon analysis suggested that the removal of quasi-periodicity is necessary to allow highly anharmonic scattering of low-frequency ( $<2\text{ THz}$ ) phonon modes, and thereby the lowest  $\kappa$ .

This study highlights the connection between  $\kappa$  and the arrangement of atoms at the nanoscale, which suggests two important considerations for future theoretical and experimental work. First, we note that previous first-principles calculations to study random alloys may have inadvertently included quasi-periodicity owing to limited supercell sizes and computational power. Therefore, more accurate first-principles calculations may require much larger supercells in order to predict the scattering of low-frequency phonon modes. In addition, it may be necessary to capture higher-order anharmonicity either through the inclusion of higher-order terms in lattice dynamics calculations or (ideally) through *ab initio* molecular dynamics simulations.

Second, we note that mechanical alloying (*e.g.*, high-energy ball milling) of Si and Ge powders is the most common approach to fabricate SiGe alloys. Depending on the processing conditions, it is possible that microsegregation occurs throughout the alloy. For example, Si or Ge particles can remain segregated into distinct domains, especially if thermal treatment does not induce sufficient atomic diffusion to create a

homogeneously random alloy. Therefore, this work provides motivation to advance current fabrication techniques for SiGe alloys in order to realize the alloy-limit of  $\kappa$ , which is important for thermoelectric applications.

### Acknowledgements

This work was supported in part by the Robert A. Welch Foundation (F-1535). Y. Lee is grateful for the scholarship from the Donald D. Harrington Fellows Program. We would also like to thank the Texas Advanced Computing Center for the use of their computing resources.

### References

- 1 J. Garg, N. Bonini, B. Kozinsky and N. Marzari, *Phys. Rev. Lett.*, 2011, **106**, 045901.
- 2 B. Abeles, *Phys. Rev.*, 1963, **131**, 1906.
- 3 M. Hu, K. P. Giapis, J. V. Goicochea, X. Zhang and D. Poulikakos, *Nano Lett.*, 2011, **11**, 618.
- 4 G. Zhang, W. Wang and X. Li, *Adv. Mater.*, 2008, **20**, 3654.
- 5 M. C. Wingert, Z. C. Y. Chen, E. Dechaumphai, J. Moon, J.-H. Kim, J. Xiang and R. Chen, *Nano Lett.*, 2011, **11**, 5507.
- 6 L. Yin, E. K. Lee, J. W. Lee, D. Whang, B. L. Choi and C. Yu, *Appl. Phys. Lett.*, 2012, **101**, 043114.
- 7 E. K. Lee, L. Yin, Y. Lee, J. W. Lee, S. J. Lee, J. Lee, S. N. Cha, D. Whang, G. S. Hwang, K. Hippalgaonkar, A. Majumdar, C. Yu, B. L. Choi, J. M. Kim and K. Kim, *Nano Lett.*, 2012, **12**, 2918.
- 8 H. Stohr and W. Klemm, *Z. Anorg. Allg. Chem.*, 1939, **241**, 305.
- 9 B. Abeles, D. S. Beers, G. D. Cody and J. P. Dismukes, *Phys. Rev.*, 1962, **125**, 44.
- 10 J. P. Dismukes, L. Ekstrom, E. F. Steigmeier, I. Kudman and D. S. Beers, *J. Appl. Phys.*, 1964, **35**, 2899.
- 11 M. C. Steele and F. D. Rosi, *J. Appl. Phys.*, 1958, **29**, 1517.
- 12 D. M. Rowe, L. W. Fu and S. G. K. Williams, *J. Appl. Phys.*, 1993, **73**, 4683.
- 13 G. Joshi, H. Lee, Y. Lan, X. Wang, G. Zhu, D. Wang, R. W. Gould, D. C. Cuff, M. Y. Tang, M. S. Dresselhaus, G. Chen and Z. Ren, *Nano Lett.*, 2008, **8**, 4670.
- 14 J. Garg, PhD thesis, MIT, 2011.
- 15 A. Kundu, N. Mingo, D. A. Broido and D. A. Stewart, *Phys. Rev. B: Condens. Matter Mater. Phys.*, 2011, **84**, 125426.
- 16 A. Skye and P. K. Schelling, *J. Appl. Phys.*, 2008, **103**, 113524.
- 17 Y. Lee and G. S. Hwang, *J. Appl. Phys.*, 2013, **114**, 174910.
- 18 Y. He, I. Savic, D. Donadio and G. Galli, *Phys. Chem. Chem. Phys.*, 2012, **14**, 16209.
- 19 C. H. Baker and P. M. Norris, *Phys. Rev. B: Condens. Matter Mater. Phys.*, 2015, **91**, 180302.
- 20 Y. Lee and G. S. Hwang, *Phys. Rev. B: Condens. Matter Mater. Phys.*, 2012, **85**, 125204.
- 21 S. Plimpton, *J. Comput. Phys.*, 1995, **117**, 1.
- 22 H. Shibata, Y. Waseda, H. Ohta, K. Kiyomi, K. Shimoyama, K. Fujito, H. Nagaoka, Y. Kagamitani, R. Simura and T. Fukuda, *Mater. Trans., JIM*, 2007, **48**, 2782.

- 23 L. Lindsay and D. A. Broido, *J. Phys.: Condens. Matter*, 2008, **20**, 165209.
- 24 L. Lindsay, D. A. Broido and T. L. Reinecke, *Phys. Rev. Lett.*, 2012, **109**, 095901.
- 25 Advances in Physics Theories and Applications, www.iiste.org, ISSN 2224-719X (paper) ISSN 2225-0638 (online) vol. 5, accessed 2013.
- 26 P. Giannozzi, S. de Gironcoli, P. Pavone and S. Baroni, *Phys. Rev. B: Condens. Matter Mater. Phys.*, 1991, **43**, 7231.
- 27 C. Kittel, *Introduction to Solid State Physics*, Wiley, New York, 7th edn, 2006.
- 28 A. J. H. McGaughey and M. Kaviani, *Phys. Rev. B: Condens. Matter Mater. Phys.*, 2004, **69**, 094303.